JACS
JOURNAL OF THE AMERICAN CHEMICAL SOCIETY

pubs.acs.org/JACS

Article

Controlled Diffusion of Photoswitchable Receptors by Binding Anti-electrostatic Hydrogen-Bonded Phosphate Oligomers

Thomas S. C. MacDonald, Ben L. Feringa, William S. Price, Sander J. Wezenberg,* and Jonathon E. Beves*

Cite This: J. Am. Chem. Soc. 2020, 142, 20014–20020

Read Online

ACCESS | Metrics & More | Article Recommendations | Supporting Information

ABSTRACT: Dihydrogen phosphate anions are found to spontaneously associate into anti-electrostatic oligomers *via* hydrogen bonding interactions at millimolar concentrations in DMSO. Diffusion NMR measurements supported formation of these oligomers, which can be bound by photoswitchable anion receptors to form large bridged assemblies of approximately three times the volume of the unbound receptor. Photoisomerization of the oligomer-bound receptor causes a decrease in diffusion coefficient of up to 16%, corresponding to a 70% increase in effective volume. This new approach to external control of diffusion opens prospects in controlling molecular transport using light.

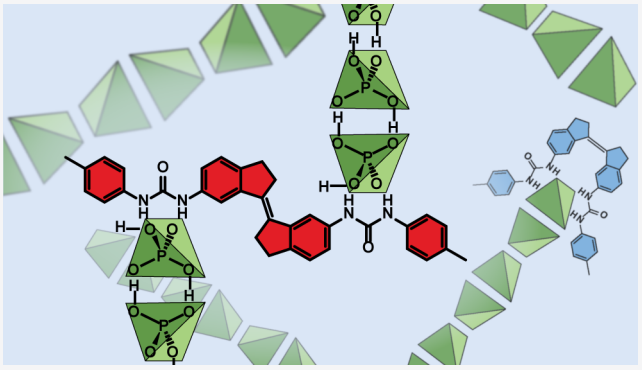

INTRODUCTION

Active control over molecular transport by synthetic systems is a topic of major contemporary interest.[1] Recent progress has shown that motors,[2] enzymes, or other energy-consuming nanostructures can effectively drive molecular transport in solution.[2b,3a−k] Despite these advances, controlling transport of molecules in solution remains a challenging goal. One way to control transport is by modulating the diffusion rate of species in solution. Various theoretical proposals and experimental data have shown that increasing or decreasing the rate of diffusion can lead to directional transport when coupled with, for example, concentration gradients.[4] Diffusion rates have been influenced using molecular photoswitches[5] by altering self-assembled discrete structures[5a,c,e,6] or polymers.[5e,6,7a,b] While diffusion NMR[8] measurements are an established approach for characterizing supramolecular assemblies,[9] the use of a switchable assembly to control diffusive transport is relatively unexplored.

Many small molecular receptors have been developed to selectively bind anions.[10] Such binding may result in changes in the rate of diffusion of the receptor. If the binding properties could be modified by external stimuli, for example, by light,[11] this could allow control of the rate of diffusion. Recently, some of us developed the first photoswitchable receptors exhibiting strong dihydrogen phosphate binding.[12] These receptors were based on molecular motor and stiff-stilbene scaffolds[13] containing urea anion-binding motifs. These hosts could be converted from a weakly guest-binding *E* to a strongly binding *Z* form using near-UV light (Figure 1a).

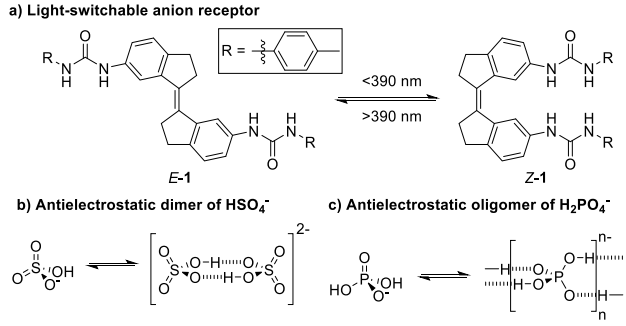

Figure 1. (a) Bis-urea anion binding photoswitch **1**. The binding of *Z*-**1** to anions is approximately oneorder of magnitude stronger than that of *E*-**1**. The photoisomers can be interconverted by irradiation with near-UV light. (b) Anti-electrostatic hydrogen bonding of anions. Anions with a single hydrogen bond donor/acceptor pair (e.g., HSO_4^-) may form dimers,[15] while (c) anions with multiple donor/acceptors (e.g., $H_2PO_4^-$) can form oligomers in the solid state.[16]

Some anions are known to associate through hydrogen bonds that are sufficiently strong to overcome electrostatic repulsion to form polyanionic species.[14] This anti-electrostatic

Received: August 24, 2020
Published: November 12, 2020

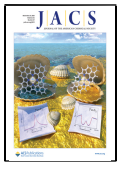

https://dx.doi.org/10.1021/jacs.0c09072
J. Am. Chem. Soc. 2020, 142, 20014−20020

hydrogen bonding (AEHB) is common in the solid state for oxoanions such as HCO_3^-, HSO_4^-, and $H_2PO_4^-$ (Figure 1b,c).

While AEHB interactions have been identified in solid-state crystal structures, detection of unchaperoned anion dimers or oligomers in solution is challenging due to limited spectroscopic signatures, weak anion−anion bonds, labile protons, and rapidly exchanging bound species. These difficulties can be attenuated by the use of an anion-binding host to template AEHB interactions,[17] leading to reports of HSO_4^- dimers[15,18] and $H_2PO_4^-$ dimers[19] and oligomers[20,16] in solution. Conductimetric and spectroscopic techniques have shown the formation of AEHB dimers of HCO_3^- and $H_2PO_4^-$ in water[21] or DMSO[22] and suggested the possibility of higher order oligomers.[21c] However, to the best of our knowledge, the unassisted formation of AEHB oxoanion oligomers in solution has yet to be conclusively established. We anticipated that the use of photoswitchable anion receptors with AEHB dihydrogen phosphate oligomers would allow changes in diffusion to be controlled by light. Herein we report quantitative self-association data for the anti-electrostatic oligomerization of dihydrogen phosphate in DMSO at millimolar concentrations, and the use of a photoswitchable anion receptor to allow reversible binding to control rates of diffusive transport.

RESULTS AND DISCUSSION

Our initial studies of tetrabutylammonium dihydrogen phosphate ($[NBu_4][H_2PO_4]$) solutions in DMSO-d_6 with 0.5% v/v added water[23] revealed a surprising decrease in the diffusion coefficient of the $H_2PO_4^-$ anion $D(H_2PO_4)$ at higher concentrations, while the diffusion coefficient of the NBu_4^+ counterion $D(NBu_4)$ remained relatively constant (Figure 2; see SI-6). This behavior cannot be explained by changes in ion pairing or viscosity which must affect the diffusion coefficients of both ions equally. Control experiments with tetrabutylammonium acetate did not show comparable continuing decreases in diffusion coefficients of either NBu_4^+ or acetate over the same concentration range as used for $[NBu_4][H_2PO_4]$ (SI-S6.1), indicating that the formation of oligomers was unique to $H_2PO_4^-$.

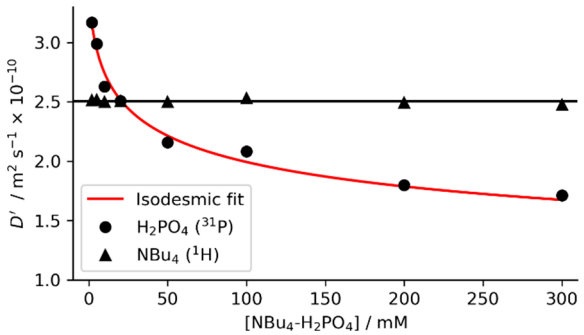

Figure 2. Diffusion coefficients of tetrabutylammonium dihydrogen phosphate ($[NBu_4][H_2PO_4]$) measured by ^{1}H (500 MHz) or ^{31}P (202 MHz) NMR over the 2−300 mM concentration range and corrected for changes in viscosity using independent viscosity measurements (see SI-S4). An isodesmic oligomerization model (eq 1, red line) was fitted to the measured diffusion coefficients of dihydrogen phosphate giving parameters $K_i = 120 \pm 32$ M^{-1} and $D_0 = 3.39 \pm 0.11 \times 10^{-10}$ m^2 s^{-1}. All measurements in DMSO-d_6 with 0.5% v/v added water. Data was processed using scripts given in SI-12.

Diffusion coefficients vary approximately proportionally to the inverse cube root of molecular volume, $V^{-1/3}$.[24] Therefore, the 50% decrease in $D(H_2PO_4)$ as the $H_2PO_4^-$ concentration is increased from 2 to 300 mM suggests an *8-fold increase* in effective volume over this concentration range. We propose this decrease in $D(H_2PO_4)$ is a result of the formation of AEHB oligomers of $H_2PO_4^-$ in solution.

A simple model for supramolecular oligomerization is the isodesmic model, in which the addition of each monomer to an oligomer occurs with the same association constant K_i (SI−S5.1).[25] Combining this model with an inverse-cube relationship between D and oligomer size (see SI−S5.2 for derivation and details) gives a model for the concentration dependence of the measured D of a molecular species undergoing reversible oligomerization:

$$\bar{D} = \frac{D_0}{K_i[A]_0}\mathrm{Li}_{-\frac{2}{3}}(K_i[A]) \qquad (1)$$

where $\mathrm{Li}_s(z)$ is the polylogarithm function,[26] D_0 is the diffusion coefficient of the monomer, K_i is the isodesmic association constant, $[A]_0$ is the total concentration, and $[A]$ is the concentration of the free (monomeric) species which can be obtained from K_i and $[A]_0$. Nonlinear regression of eq 1 onto the measured diffusion coefficients of $H_2PO_4^-$ gave $K_i = 120 \pm 32$ M^{-1}, surprisingly close to the reported dimerization constants of $H_2PO_4^-$ in pure DMSO (180 M^{-1} measured by ^{31}P NMR,[22] 51 M^{-1} measured by ITC[17]). Our measured K_i corresponds to median complexes composed of 4 or 10 $H_2PO_4^-$ subunits at 50 or 300 mM concentrations, respectively (Figure 3a, Figure S11), and as far as we know, this surprisingly strong process in a polar solvent is the first measurement of indefinite AEHB self-association. This model makes no assumptions about the structure of the self-assembly, which could be, for example, linear chains or globular-type assemblies, as suggested by the diversity of known solid-state structures containing $H_2PO_4^-$ clusters.[27]

To modify the diffusion rate of a switchable receptor, we turned to the previously developed stiff stilbene,[5c,e] bis-urea.[12c,e] The bis-tolyl derivative **1** (Figure 1a) was synthesized to take advantage of the convenient methyl ^{1}H NMR signal for diffusion NMR experiments (see SI-3). The association constants for $H_2PO_4^-$ and OAc^- were measured by NMR titrations and fitted to 1:2 $[HG_2]$ binding models, with results[28] comparable to those previously reported for the nonsubstituted phenyl derivative[12c] when studied over the same guest concentration range. Binding studies at higher concentrations of $H_2PO_4^-$, however, resulted in slightly different association constants when fitted to the same binding model (SI-S7.8−7.10) illustrating that competition due to self-association of $H_2PO_4^-$ complicates binding models for association constants.[29] For example, a recent report of $H_2PO_4^-$ binding[30] found different binding constants and stoichiometries when measured at different concentrations by UV−vis absorption or NMR spectroscopy, likely due to $H_2PO_4^-$ aggregation. This problem will also apply to all other $H_2PO_4^-$ binding studies measured at millimolar or higher concentrations.

The photoswitching properties of **1** were studied in DMSO-d_6 with 0.5% v/v added water,[12c] and absorption spectra (Figure S45) are in line with the parent compound.[12c] The thermal half-life is sufficiently long that no thermal isomerization was observable over the time scales used in the

https://dx.doi.org/10.1021/jacs.0c09072
J. Am. Chem. Soc. 2020, 142, 20014−20020

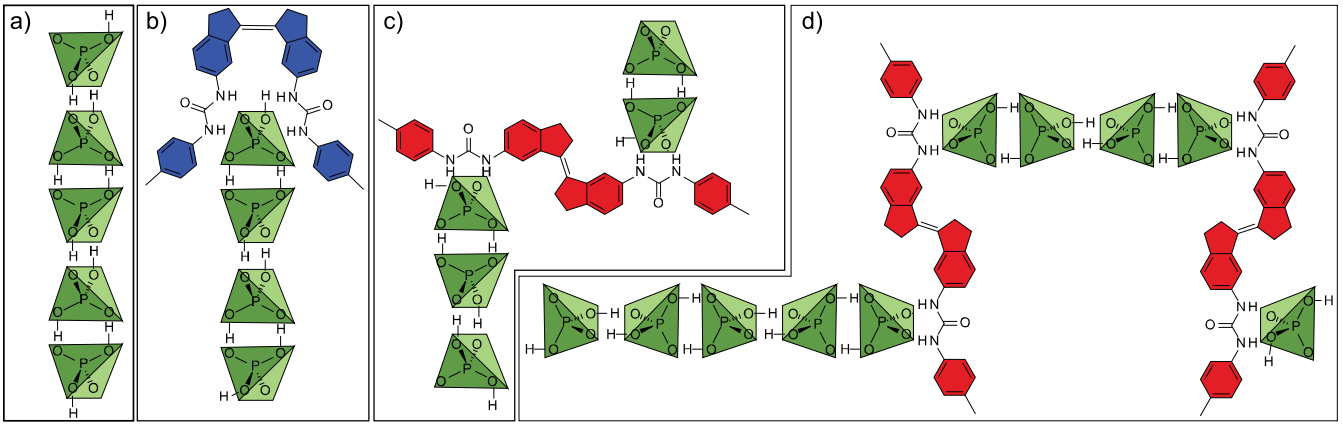

Figure 3. Example supramolecular assemblies present in solution. (a) Anti-electrostatic dihydrogen phosphate ($H_2PO_4^-$) oligomers, G_n, form from monomeric phosphates. These oligomers are bound by anion-binding *Z*-**1** (b) and *E*-**1** (c) bis-urea hosts to form ditopic [H(G_n)] or [H(G_n)$_2$] complexes. (d) As *E*-**1** possesses divergent urea binding sites, larger supramolecular structures can form from $H_2PO_4^-$ chains linked by *E*-**1** hosts.

Table 1. Changes in Diffusion Coefficients of Pure Isomers and 1:1 Mixed Solutions of *E*-1 and *Z*-1 in the Presence of 50 mM NBu_4−H_2PO_4[a]

entry	[$H_2PO_4^-$] (mM)	[*E*-**1**] (mM)	[*Z*-**1**] (mM)	$D(H_2PO_4)$[b]/10^{-10} (m^2 s^{-1})	D(*E*-**1**)[c]/10^{-10} (m^2 s^{-1})	D(*Z*-**1**)[c]/10^{-10} (m^2 s^{-1})	$D(NBu_4)$[c]/10^{-10} (m^2 s^{-1})
1		5			1.74 ± 0.03		
2			5			1.87 ± 0.01	
3	50			2.16 ± 0.03			2.50 ± 0.02
4	50	5		1.93 ± 0.04	1.17 ± 0.03		2.39 ± 0.01
5	50		5	2.01 ± 0.03		1.39 ± 0.01	2.37 ± 0.02
6	50	5	5	1.83 ± 0.08	1.12 ± 0.02	1.36 ± 0.01	2.31 ± 0.01
7	50	2.5	2.5	1.97 ± 0.07	1.19 ± 0.01	1.45 ± 0.03	2.44 ± 0.01
8	50	0.5	0.5	2.05 ± 0.02	1.27 ± 0.03	1.57 ± 0.03	2.52 ± 0.02

[a]DMSO-d_6 with 0.5% v/v added water. [b]202 MHz ^{31}P PGSTE, δ = 7 ms, Δ = 100 ms, g = 0−53.5 G cm^{-1}. [c]500 MHz ^{1}H PGSTE, δ = 4 ms, Δ = 50 ms, g = 0−53.5 G cm^{-1}.

experiments reported here. In the presence of 50 mM [NBu_4][H_2PO_4], the photostationary state under nonoptimal irradiation with a 405 nm LED comprised a *E*/*Z* ratio of 58:42 as measured by NMR integration.

The measured diffusion coefficients of *E*-**1** and *Z*-**1** (D(*E*-**1**) and D(*Z*-**1**)) in DMSO-d_6 with 0.5% v/v added water are shown in Table 1. In the absence of $H_2PO_4^-$, the extended *E*-**1** isomer diffuses slightly more slowly (7%) than the more compact *Z*-**1** (Table 1; entry 1 vs 2). Given the large difference in size between host **1** (MW = 529, approximately longest axis 13 Å) and the $H_2PO_4^-$ anion (MW = 97, radius 2.5 Å),[31] we might have anticipated a modest decrease in average host diffusion coefficients at guest concentrations where near-complete complexation occurs based on measured binding constants.[32]

Instead, we observe a large decrease in measured D(**1**) that continues to decrease at concentrations above those predicted for near-complete complexation.[33] After correcting for $H_2PO_4^-$ induced viscosity changes (see SI-4),[34] the measured D of pure *E*-**1** or *Z*-**1** in the presence of 50 mM [NBu_4][H_2PO_4] was found to decrease by 33% (D(*E*-**1**)) or 26% (D(*Z*-**1**)) relative to D without [NBu_4][H_2PO_4] (Table 1; entries 1 vs 4; 2 vs 5; Figure 4 for full [$H_2PO_4^-$]-dependent diffusion data). This suggests greater than 2 or 3-fold increases in effective volumes of the *Z*-**1** or *E*-**1** hosts, respectively. These substantial decreases in measured D are too large to be explained by the formation of simple ditopic [HG_2] complexes[12c] or even [H(G_n)$_2$] complexes, where G_n is an oligomeric assembly of *n* hydrogen-bonded $H_2PO_4^-$ subunits that forms as in the absence of host[35] (Figure 3b,c see Figure S11 for modeling).[12c]

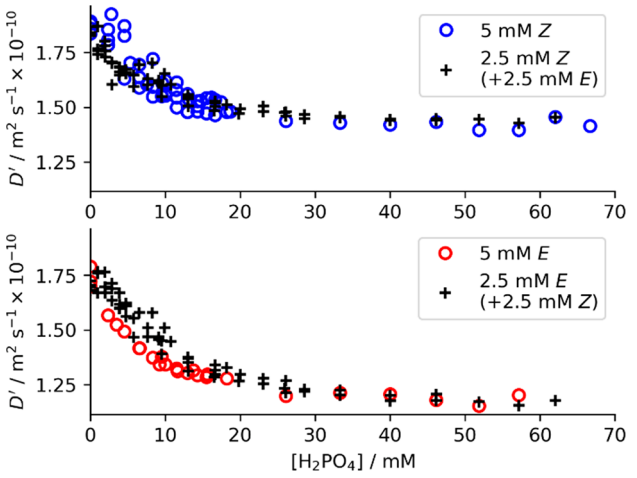

Figure 4. Diffusion measurements of hosts *Z*-**1** and *E*-**1** under titration with [NBu_4][H_2PO_4]. Measured D for 5 mM solutions of pure *Z*-**1** or *E*-**1** (○), compared with mixed 2.5 mM/2.5 mM *E*-**1**/*Z*-**1** (+).

Host *E*-**1** forms larger structures than host *Z*-**1**, despite having a lower binding constant.[36] This observation is also supported by changes in the measured diffusion of $H_2PO_4^-$, $D(H_2PO_4)$, (measured by ^{31}P NMR), which decreases by 11% or 7% in the presence of 5 mM of *E*-**1** or *Z*-**1**, respectively

https://dx.doi.org/10.1021/jacs.0c09072
J. Am. Chem. Soc. 2020, 142, 20014−20020

(Table 1; entries 3 vs 4, 5). This indicates that $H_2PO_4^-$ is also assembled into larger average structures in the presence of *E*-**1** than in the presence of *Z*-**1**.

The D(*E*-**1**) and D(*Z*-**1**) measured in 5 mM solutions of a single isomer of **1** decrease by just 4% and 2%, respectively, when a 5 mM amount of the other isomer is also present (Table 1; entries 4 vs 6; 5 vs 6), suggesting minimal interactions between the *E*- and *Z*-isomers.

Relative to that of a solution of pure $[NBu_4][H_2PO_4]$, $D(H_2PO_4)$ decreases on going from 5 mM *Z*-**1** (−7%, Table 1, entry 5) to 5 mM *E*-**1** (−11%, entry 4) to 5 mM *Z*-**1** and *E*-**1** (−15%, entry 6). $D(H_2PO_4)$ for a solution of 2.5 mM *E*-**1** and 2.5 mM *Z*-**1** (−9%, entry 7) is also the average of that 5 mM solutions of each isomer (entries 4, 5). This also suggests the $H_2PO_4^-$ does not experience anything other than a statistical binding by the hosts, with surprisingly no evidence of cross-linking between different host isomers.

However, there is evidence that complexes are formed involving multiple host molecules of the same isomer. To test this, titration experiments with $[NBu_4][H_2PO_4]$ were conducted with solutions of 1:1 mixtures of *E*-**1**:*Z*-**1** at 1, 5, and 10 mM total concentrations (SI-8.3). A small but observable decrease in D for both *E*-**1** and *Z*-**1** was found as the total concentration of the host increased from 1 to 5 to 10 mM (e.g., at 50 mM $[NBu_4][H_2PO_4]$: Table 1, entries 6−8; also SI−S8.3). This data supports the formation of structures involving multiple hosts, such as structures such as shown in Figure 3d.

Host **1** could also increase the effective size of polyanionic complexes by increasing ion pairing to the NBu_4^+ cations. This would result in a decrease in $D(NBu_4)$ with increasing host concentration, but only a 5% decrease in $D(NBu_4)$ is observed (Table 1, entry 3 vs 4; 3 vs 5), suggesting ion pairing is only a minor contributor. There is also no difference between $D(NBu_4)$ in the presence of *E*-**1** or *Z*-**1**, despite *E*-**1** forming much larger complexes (Table 1; entries 4 vs 5). These observations suggest the hosts do not significantly change ion pairing between the NBu_4^+ and oligomers of $H_2PO_4^-$.

From the measured diffusion coefficients of free host (5 mM) and oligomeric $H_2PO_4^-$ (50 mM), we estimate the assemblies formed involve 1−2 molecules of **1** with 2−3 assemblies of oligomeric guest G_n, (where n is the same as that formed at 50 mM $[NBu_4][H_2PO_4]$ in the absence of host, see SI−S9 for discussion of methodology).[37] From the modeled size distribution of $H_2PO_4^-$ oligomers at 50 mM (Figure S11), this corresponds to complexes incorporating approximately 10 $H_2PO_4^-$ subunits with average molecular weights of 1.5−2.0 kDa. Together, these results indicate that $H_2PO_4^-$ anions not only form aggregates in polar and hydrogen-bond accepting solvents, but that these structures can associate to form larger assemblies with multiple hosts in solution.

As host **1** is a photoswitch, the *E*-**1**/*Z*-**1** distribution of isomers can be controlled using light (SI-10). Reversible switching was investigated by UV−vis absorption; see Figure S46. By combining *in situ* irradiation within the NMR spectrometer[38] with recently developed time-resolved diffusion NMR techniques,[39] we simultaneously measured changes in concentration and diffusion coefficients of *E*-**1** and *Z*-**1** under 400 nm irradiation (Figure 5). The rapidly changing concentration during the early stages of the reaction causes the observed noise; see SI-S10.2 for more details.

Photoswitching of organic molecules is expected to result in differences in D, but such changes would typically be minor

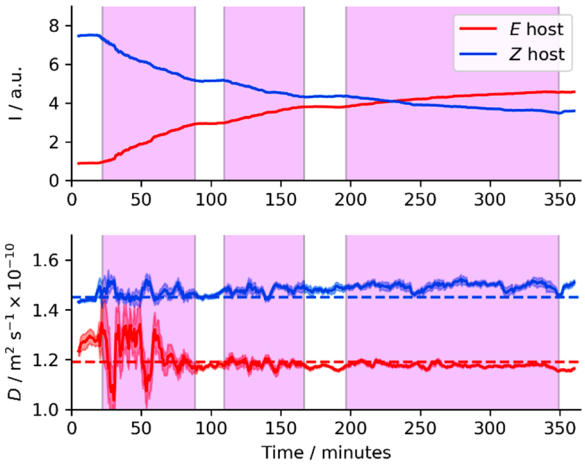

Figure 5. Photoswitching of *Z*-**1** host in the presence of 50 mM $H_2PO_4^-$ under in situ irradiation with 400 nm light (shaded purple areas). Concentrations (top) and diffusion coefficients (bottom) were monitored simultaneously using time-resolved diffusion NMR.[39a,c] Lines and shaded areas on diffusion subplot are respectively values and errors from the Stejskal−Tanner fit. Dashed horizontal lines show measured D(*E*-**1**) and D(*Z*-**1**) for a 5 mM 1:1 mixture of isomers (Table 1, entry 7). 500 MHz ^{1}H, δ = 4 ms, Δ = 50 ms, g = 0−53.45 G cm^{-1}, DMSO-d_6 with 0.5% v/v added water and glass capillaries used to suppress convection.[40] See Figure S44 for data with in situ temperature measurements and Figure S46 for demonstration of reversibility of switching.[39c,41]

(e.g., the 7% difference between D(*E*-**1**) and D(*Z*-**1**) in the absence of anion guest (Table 1, entries 1 and 2). Switchable anion binding might give more control over the effective host D, but complexes with small anions (e.g., Cl^-, OAc^-, NO_3^-, HSO_4^-) might only cause modest changes in host D, as found for control experiments with acetate (8% and 4% decrease, respectively, in D(*E*-**1**) and D(*Z*-**1**) at 50 mM $[NBu_4][OAc]$; SI-S8.2). The use of $H_2PO_4^-$ oligomers allows greater control over D: switching host **1** from *Z*-**1** to *E*-**1** causes a "molecular gear change" and a 16% decrease in measured D (Table 1, entries 4 and 5), suggestive of an approximately 70% increase in average molecular volume. This demonstrates substantial control over the diffusion rate of small molecules in bulk solution by coupling photocontrol of guest-binding to the ability of $H_2PO_4^-$ to form extended supramolecular structures.[42] As **1** is a thermally stable ("P-type") photoswitch,[5e,h] these changes in D will persist in the dark.

CONCLUSION

In conclusion, we sought to use the switchable anion-binding properties of host **1** to achieve photocontrol of translational diffusion rates. Diffusion NMR allowed characterization of the thermodynamics of the anti-electrostatic self-assembly of the bare dihydrogen phosphate anion in solution, a long-suspected[21a,b] but previously uncharacterized phenomenon. We obtained a surprisingly high isodesmic association constant of K_i = 120 ± 32 M^{-1} for $H_2PO_4^-$ self-association, which corresponds to complexes of a median size of four (or 10) $H_2PO_4^-$ subunits at concentrations of 50 mM (or 300 mM) in wet DMSO. Anion binding studies with $H_2PO_4^-$ in DMSO therefore always involve competition between host−$H_2PO_4^-$ and $H_2PO_4^-$−$H_2PO_4^-$ interactions,[14h,17] which poses problems for fitting titration data (SI-7.11 for further discussion). Because of the limited solubility of our bis-urea receptor, this

https://dx.doi.org/10.1021/jacs.0c09072
J. Am. Chem. Soc. 2020, 142, 20014−20020

study was conducted exclusively in wet DMSO. It would be reasonable to assume that in less polar solvents such as DMF, acetonitrile, or dichloromethane self-association of $H_2PO_4^-$ may be more significant. To test this, we measured the diffusion coefficients of $[NBu_4][H_2PO_4]$ in $CDCl_3$. Due to tight ion pairing the diffusion coefficients of the cation and anion were close over the range of 2−300 mM. A decrease in $D(H_2PO_4)$ of around 40% is observed over this concentration range, consistent with the formation of oligomers similar to that observed in DMSO-d_6 (see SI-12 for details). This result suggests ion pairing may disrupt the formation of even larger oligomers in noncompetitive solvents.

Combining the unusual anti-electrostatic oligomerization of $H_2PO_4^-$ with a photoswitchable anion-binding receptor allowed light to induce a "gear change" and sharply change the rate of receptor diffusion, equivalent to a 70% change in effective volume. Can control of diffusion *via* a spatially selective stimulus (such as light, as demonstrated here) drive directional transport of small molecular species and create concentration gradients? This remains an interesting open question.

■ ASSOCIATED CONTENT

Supporting Information

The Supporting Information is available free of charge at https://pubs.acs.org/doi/10.1021/jacs.0c09072.

Experimental procedures, NMR spectra, scripts used to process diffusion NMR data (PDF)

■ AUTHOR INFORMATION

Corresponding Authors

Jonathon E. Beves − *School of Chemistry, University of New South Wales, Sydney, NSW 2052, Australia;* orcid.org/0000-0002-5997-6580; Email: j.beves@unsw.edu.au

Sander J. Wezenberg − *Leiden Institute of Chemistry, Leiden University, 2333 CC Leiden, The Netherlands;* orcid.org/0000-0001-9192-3393; Email: s.j.wezenberg@lic.leidenuniv.nl

Authors

Thomas S. C. MacDonald − *School of Chemistry, University of New South Wales, Sydney, NSW 2052, Australia;* orcid.org/0000-0002-2219-6759

Ben L. Feringa − *Stratingh Institute for Chemistry, University of Groningen, 9747, AG, Groningen, The Netherlands;* orcid.org/0000-0003-0588-8435

William S. Price − *School of Science, Western Sydney University, Penrith, NSW 2751, Australia;* orcid.org/0000-0002-8549-4665

Complete contact information is available at: https://pubs.acs.org/10.1021/jacs.0c09072

Notes

The authors declare no competing financial interest.

Raw experimental data has been deposited on ChemRxiv and is available at DOI: 10.26434/chemrxiv.12298919.v1.

■ ACKNOWLEDGMENTS

We thank Prof. Tim Schmidt, Prof. Palli Thordarson, and Prof. Amar Flood for fruitful discussions. The Australian Research Council (JEB, FT170100094), the Australian Government (TSCM, Australian Postgraduate Award), the Ministry of Education, Culture and Science (Gravitation Program 024.001.035), and the European Research Council (Advanced Grant no. 694345 to B.L.F. and Starting Grant no. 802830 to S.J.W.) are acknowledged for funding. We acknowledge the Mark Wainwright Analytical Centre at UNSW Sydney for access to the NMR facility.

■ REFERENCES

(1) (a) Kay, E. R.; Leigh, D. A.; Zerbetto, F. Synthetic Molecular Motors and Mechanical Machines. *Angew. Chem., Int. Ed.* **2007**, *46*, 72−191. (b) Hänggi, P.; Marchesoni, F. Artificial Brownian motors: Controlling transport on the nanoscale. *Rev. Mod. Phys.* **2009**, *81*, 387−442. (c) Lauga, E.; Powers, T. R. The hydrodynamics of swimming microorganisms. *Rep. Prog. Phys.* **2009**, *72*, 096601. (d) Sengupta, S.; Ibele, M. E.; Sen, A. Fantastic Voyage: Designing Self-Powered Nanorobots. *Angew. Chem., Int. Ed.* **2012**, *51*, 8434−8445. (e) Kapral, R. Perspective: Nanomotors without moving parts that propel themselves in solution. *J. Chem. Phys.* **2013**, *138*, 020901. (f) Ma, X.; Hahn, K.; Sanchez, S. Catalytic Mesoporous Janus Nanomotors for Active Cargo Delivery. *J. Am. Chem. Soc.* **2015**, *137*, 4976−4979. (g) Sanchez, S.; Soler, L.; Katuri, J. Chemically Powered Micro- and Nanomotors. *Angew. Chem., Int. Ed.* **2015**, *54*, 1414−1444.

(2) (a) Browne, W. R.; Feringa, B. L. Making molecular machines work. *Nat. Nanotechnol.* **2006**, *1*, 25−35. (b) Kudernac, T.; Ruangsupapichat, N.; Parschau, M.; Maciá, B.; Katsonis, N.; Harutyunyan, S. R.; Ernst, K.-H.; Feringa, B. L. Electrically driven directional motion of a four-wheeled molecule on a metal surface. *Nature* **2011**, *479*, 208−211. (c) Feringa, B. L. The Art of Building Small: From Molecular Switches to Motors (Nobel Lecture). *Angew. Chem., Int. Ed.* **2017**, *56*, 11060−11078.

(3) (a) Heureux, N.; Lusitani, F.; Browne, W. R.; Pshenichnikov, M. S.; van Loosdrecht, P. H. M.; Feringa, B. L. Following the Autonomous Movement of Silica Microparticles Using Fluorescence Microscopy. *Small* **2008**, *4*, 476−480. (b) Pantarotto, D.; Browne, W. R.; Feringa, B. L. Autonomous propulsion of carbon nanotubes powered by a multienzyme ensemble. *Chem. Commun.* **2008**, 1533−1535. (c) Stock, C.; Heureux, N.; Browne, W. R.; Feringa, B. L. Autonomous Movement of Silica and Glass Micro-Objects Based on a Catalytic Molecular Propulsion System. *Chem. - Eur. J.* **2008**, *14*, 3146−3153. (d) Wilson, D. A.; Nolte, R. J. M.; van Hest, J. C. M. Autonomous movement of platinum-loaded stomatocytes. *Nat. Chem.* **2012**, *4*, 268−274. (e) García-López, V.; Chiang, P.-T.; Chen, F.; Ruan, G.; Martí, A. A.; Kolomeisky, A. B.; Wang, G.; Tour, J. M. Unimolecular Submersible Nanomachines. Synthesis, Actuation, and Monitoring. *Nano Lett.* **2015**, *15*, 8229−8239. (f) Lozano, C.; ten Hagen, B.; Löwen, H.; Bechinger, C. Phototaxis of synthetic microswimmers in optical landscapes. *Nat. Commun.* **2016**, *7*, 12828. (g) Yao, X.; Li, T.; Wang, J.; Ma, X.; Tian, H. Recent Progress in Photoswitchable Supramolecular Self-Assembling Systems. *Adv. Opt. Mater.* **2016**, *4*, 1322−1349. (h) Katuri, J.; Ma, X.; Stanton, M. M.; Sánchez, S. Designing Micro- and Nanoswimmers for Specific Applications. *Acc. Chem. Res.* **2017**, *50*, 2−11. (i) Zhao, X.; Gentile, K.; Mohajerani, F.; Sen, A. Powering Motion with Enzymes. *Acc. Chem. Res.* **2018**, *51*, 2373−2381. (j) Tu, Y.; Peng, F.; Heuvelmans, J. M.; Liu, S.; Nolte, R. J. M.; Wilson, D. A. Motion Control of Polymeric Nanomotors Based on Host−Guest Interactions. *Angew. Chem., Int. Ed.* **2019**, *58*, 8687−8691. (k) Fernández-Medina, M.; Ramos-Docampo, M. A.; Hovorka, O.; Salgueiriño, V.; Städler, B. Recent Advances in Nano- and Micromotors. *Adv. Funct. Mater.* **2020**, *30*, 1908283.

(4) (a) Anderson, J. L.; Prieve, D. C. Diffusiophoresis caused by gradients of strongly adsorbing solutes. *Langmuir* **1991**, *7*, 403−406. (b) Astumian, R. D. Enhanced Diffusion, Chemotaxis, and Pumping by Active Enzymes: Progress toward an Organizing Principle of Molecular Machines. *ACS Nano* **2014**, *8*, 11917−11924. (c) Agudo-Canalejo, J.; Adeleke-Larodo, T.; Illien, P.; Golestanian, R. Enhanced Diffusion and Chemotaxis at the Nanoscale. *Acc. Chem. Res.* **2018**, *51*,

2365−2372. (d) Weistuch, C.; Pressé, S. Spatiotemporal Organization of Catalysts Driven by Enhanced Diffusion. *J. Phys. Chem. B* **2018**, *122*, 5286−5290. (e) Sear, R. P. Diffusiophoresis in Cells: A General Nonequilibrium, Nonmotor Mechanism for the Metabolism-Dependent Transport of Particles in Cells. *Phys. Rev. Lett.* **2019**, *122*, 128101.

(5) (a) Rakotondradany, F.; Whitehead, M. A.; Lebuis, A.-M.; Sleiman, H. F. Photoresponsive Supramolecular Systems: Self-Assembly of Azodibenzoic Acid Linear Tapes and Cyclic Tetramers. *Chem. - Eur. J.* **2003**, *9*, 4771−4780. (b) Lee, S.; Oh, S.; Lee, J.; Malpani, Y.; Jung, Y.-S.; Kang, B.; Lee, J. Y.; Ozasa, K.; Isoshima, T.; Lee, S. Y.; Hara, M.; Hashizume, D.; Kim, J.-M. Stimulus-Responsive Azobenzene Supramolecules: Fibers, Gels, and Hollow Spheres. *Langmuir* **2013**, *29*, 5869−5877. (c) Xu, J.-F.; Chen, Y.-Z.; Wu, D.; Wu, L.-Z.; Tung, C.-H.; Yang, Q.-Z. Photoresponsive Hydrogen-Bonded Supramolecular Polymers Based on a Stiff Stilbene Unit. *Angew. Chem., Int. Ed.* **2013**, *52*, 9738−9742. (d) van Herpt, J. T.; Areephong, J.; Stuart, M. C. A.; Browne, W. R.; Feringa, B. L. Light-Controlled Formation of Vesicles and Supramolecular Organogels by a Cholesterol-Bearing Amphiphilic Molecular Switch. *Chem. - Eur. J.* **2014**, *20*, 1737−1742. (e) Yan, X.; Xu, J.-F.; Cook, T. R.; Huang, F.; Yang, Q.-Z.; Tung, C.-H.; Stang, P. J. Photoinduced transformations of stiff-stilbene-based discrete metallacycles to metallosupramolecular polymers. *Proc. Natl. Acad. Sci. U. S. A.* **2014**, *111*, 8717−8722. (f) McConnell, A. J.; Wood, C. S.; Neelakandan, P. P.; Nitschke, J. R. Stimuli-Responsive Metal−Ligand Assemblies. *Chem. Rev.* **2015**, *115*, 7729−7793. (g) Yang, L.; Tan, X.; Wang, Z.; Zhang, X. Supramolecular Polymers: Historical Development, Preparation, Characterization, and Functions. *Chem. Rev.* **2015**, *115*, 7196−7239. (h) Kuwahara, S.; Suzuki, Y.; Sugita, N.; Ikeda, M.; Nagatsugi, F.; Harada, N.; Habata, Y. Thermal *E*/*Z* Isomerization in First Generation Molecular Motors. *J. Org. Chem.* **2018**, *83*, 4800−4804.

(6) Han, M.; Luo, Y.; Damaschke, B.; Gómez, L.; Ribas, X.; Jose, A.; Peretzki, P.; Seibt, M.; Clever, G. H. Light-Controlled Interconversion between a Self-Assembled Triangle and a Rhombicuboctahedral Sphere. *Angew. Chem., Int. Ed.* **2016**, *55*, 445−449.

(7) (a) Sun, S.-S.; Anspach, J. A.; Lees, A. J. Self-Assembly of Transition-Metal-Based Macrocycles Linked by Photoisomerizable Ligands: Examples of Photoinduced Conversion of Tetranuclear−Dinuclear Squares. *Inorg. Chem.* **2002**, *41*, 1862−1869. (b) Chen, S.; Chen, L.-J.; Yang, H.-B.; Tian, H.; Zhu, W. Light-Triggered Reversible Supramolecular Transformations of Multi-Bisthienylethene Hexagons. *J. Am. Chem. Soc.* **2012**, *134*, 13596−13599.

(8) (a) Stilbs, P. Fourier transform pulsed-gradient spin-echo studies of molecular diffusion. *Prog. Nucl. Magn. Reson. Spectrosc.* **1987**, *19*, 1−45. (b) Price, W. S. Pulsed-field gradient nuclear magnetic resonance as a tool for studying translational diffusion: Part 1. Basic theory. *Concepts Magn. Reson.* **1997**, *9*, 299−336. (c) Price, W. S. Pulsed-field gradient nuclear magnetic resonance as a tool for studying translational diffusion: Part II. Experimental aspects. *Concepts Magn. Reson.* **1998**, *10*, 197−237. (d) Johnson, C. S. Diffusion ordered nuclear magnetic resonance spectroscopy: principles and applications. *Prog. Nucl. Magn. Reson. Spectrosc.* **1999**, *34*, 203−256. (e) Callaghan, P. T. *Translational Dynamics and Magnetic Resonance: Principles of Pulsed Gradient Spin Echo NMR*; Oxford University Press, 2011.

(9) (a) Cohen, Y.; Avram, L.; Frish, L. Diffusion NMR Spectroscopy in Supramolecular and Combinatorial Chemistry: An Old Parameter—New Insights. *Angew. Chem., Int. Ed.* **2005**, *44*, 520−554. (b) Zayed, J. M.; Biedermann, F.; Rauwald, U.; Scherman, O. A. Probing cucurbit[8]uril-mediated supramolecular block copolymer assembly in water using diffusion NMR. *Polym. Chem.* **2010**, *1*, 1434−1436. (c) Li, S.-L.; Xiao, T.; Hu, B.; Zhang, Y.; Zhao, F.; Ji, Y.; Yu, Y.; Lin, C.; Wang, L. Formation of polypseudorotaxane networks by cross-linking the quadruple hydrogen bonded linear supramolecular polymersviabisparaquat molecules. *Chem. Commun.* **2011**, *47*, 10755−10757. (d) Liu, Y.; Wang, Z.; Zhang, X. Characterization of supramolecular polymers. *Chem. Soc. Rev.* **2012**, *41*, 5922−5932. (e) Avram, L.; Cohen, Y. Diffusion NMR of molecular cages and capsules. *Chem. Soc. Rev.* **2015**, *44*, 586−602. (f) Sian, L.; Guerriero, A.; Peruzzini, M.; Zuccaccia, C.; Gonsalvi, L.; Macchioni, A. Diffusion NMR Studies on the Self-Aggregation of Ru-Arene CAP Complexes: Evidence for the Formation of H-Bonded Dicationic Species in Acetonitrile. *Organometallics* **2020**, *39*, 941−948.

(10) (a) Gale, P. A.; Howe, E. N. W.; Wu, X. Anion Receptor Chemistry. *Chem.* **2016**, *1*, 351−422. (b) Chen, L.; Berry, S. N.; Wu, X.; Howe, E. N. W.; Gale, P. A. Advances in Anion Receptor Chemistry. *Chem.* **2020**, *6*, 61−141.

(11) (a) Russew, M.-M.; Hecht, S. Photoswitches: From Molecules to Materials. *Adv. Mater.* **2010**, *22*, 3348−3360. (b) Brieke, C.; Rohrbach, F.; Gottschalk, A.; Mayer, G.; Heckel, A. Light-Controlled Tools. *Angew. Chem., Int. Ed.* **2012**, *51*, 8446−8476. (c) Zhang, J.; Zou, Q.; Tian, H. Photochromic Materials: More Than Meets The Eye. *Adv. Mater.* **2013**, *25*, 378−399. (d) Göstl, R.; Senf, A.; Hecht, S. Remote-controlling chemical reactions by light: Towards chemistry with high spatio-temporal resolution. *Chem. Soc. Rev.* **2014**, *43*, 1982−1996. (e) Erbas-Cakmak, S.; Leigh, D. A.; McTernan, C. T.; Nussbaumer, A. L. Artificial Molecular Machines. *Chem. Rev.* **2015**, *115*, 10081−10206. (f) O'Hagan, M. P.; Haldar, S.; Duchi, M.; Oliver, T. A. A.; Mulholland, A. J.; Morales, J. C.; Galan, M. C. A Photoresponsive Stiff-Stilbene Ligand Fuels the Reversible Unfolding of G-Quadruplex DNA. *Angew. Chem., Int. Ed.* **2019**, *58*, 4334−4338.

(12) (a) Wezenberg, S. J.; Vlatković, M.; Kistemaker, J. C. M.; Feringa, B. L. Multi-State Regulation of the Dihydrogen Phosphate Binding Affinity to a Light- and Heat-Responsive Bis-Urea Receptor. *J. Am. Chem. Soc.* **2014**, *136*, 16784−16787. (b) Vlatković, M.; Feringa, B. L.; Wezenberg, S. J. Dynamic Inversion of Stereoselective Phosphate Binding to a Bisurea Receptor Controlled by Light and Heat. *Angew. Chem., Int. Ed.* **2016**, *55*, 1001−1004. (c) Wezenberg, S. J.; Feringa, B. L. Photocontrol of Anion Binding Affinity to a Bis-urea Receptor Derived from Stiff-Stilbene. *Org. Lett.* **2017**, *19*, 324−327. (d) Wezenberg, S. J.; Feringa, B. L. Supramolecularly directed rotary motion in a photoresponsive receptor. *Nat. Commun.* **2018**, *9*, 1984. (e) de Jong, J.; Feringa, B. L.; Wezenberg, S. J. Light-Modulated Self-Blockage of a Urea Binding Site in a Stiff-Stilbene Based Anion Receptor. *ChemPhysChem* **2019**, *20*, 3306−3310.

(13) Villarón, D.; Wezenberg, S. J. Stiff-Stilbene Photoswitches: From Fundamental Studies to Emergent Applications. *Angew. Chem., Int. Ed.* **2020**, *59*, 13192−13202.

(14) (a) Mata, I.; Alkorta, I.; Molins, E.; Espinosa, E. Electrostatics at the Origin of the Stability of Phosphate-Phosphate Complexes Locked by Hydrogen Bonds. *ChemPhysChem* **2012**, *13*, 1421−1424. (b) Weinhold, F.; Klein, R. A. Anti-Electrostatic Hydrogen Bonds. *Angew. Chem., Int. Ed.* **2014**, *53*, 11214−11217. (c) Mata, I.; Molins, E.; Alkorta, I.; Espinosa, E. The Paradox of Hydrogen-Bonded Anion−Anion Aggregates in Oxoanions: A Fundamental Electrostatic Problem Explained in Terms of Electrophilic···Nucleophilic Interactions. *J. Phys. Chem. A* **2015**, *119*, 183−194. (d) Liu, Y.; Sengupta, A.; Raghavachari, K.; Flood, A. H. Anion Binding in Solution: Beyond the Electrostatic Regime. *Chem.* **2017**, *3*, 411−427. (e) He, Q.; Tu, P.; Sessler, J. L. Supramolecular Chemistry of Anionic Dimers, Trimers, Tetramers, and Clusters. *Chem.* **2018**, *4*, 46−93. (f) Wang, C.; Fu, Y.; Zhang, L.; Danovich, D.; Shaik, S.; Mo, Y. Hydrogen- and Halogen-Bonds between Ions of like Charges: Are They Anti-Electrostatic in Nature? *J. Comput. Chem.* **2018**, *39*, 481−487. (g) Weinhold, F. Theoretical Prediction of Robust Second-Row Oxyanion Clusters in the Metastable Domain of Antielectrostatic Hydrogen Bonding. *Inorg. Chem.* **2018**, *57*, 2035−2044. (h) Zhao, W.; Flood, A. H.; White, N. G. Recognition and applications of anion−anion dimers based on anti-electrostatic hydrogen bonds (AEHBs). *Chem. Soc. Rev.* **2020**, DOI: 10.1039/D0CS00486C.

(15) Fatila, E. M.; Twum, E. B.; Sengupta, A.; Pink, M.; Karty, J. A.; Raghavachari, K.; Flood, A. H. Anions Stabilize Each Other inside Macrocyclic Hosts. *Angew. Chem., Int. Ed.* **2016**, *55*, 14057−14062.

(16) Fatila, E. M.; Pink, M.; Twum, E. B.; Karty, J. A.; Flood, A. H. Phosphate−phosphate oligomerization drives higher order co-assemblies with stacks of cyanostar macrocycles. *Chem. Sci.* **2018**, *9*, 2863−2872.

https://dx.doi.org/10.1021/jacs.0c09072
J. Am. Chem. Soc. 2020, 142, 20014−20020

(17) Bregović, N.; Cindro, N.; Frkanec, L.; Užarević, K.; Tomišić, V. Thermodynamic Study of Dihydrogen Phosphate Dimerisation and Complexation with Novel Urea- and Thiourea-Based Receptors. *Chem. - Eur. J.* **2014**, *20*, 15863−15871.
(18) (a) Fatila, E. M.; Twum, E. B.; Karty, J. A.; Flood, A. H. Ion Pairing and Co-facial Stacking Drive High-Fidelity Bisulfate Assembly with Cyanostar Macrocyclic Hosts. *Chem. - Eur. J.* **2017**, *23*, 10652−10662. (b) Barišić, D.; Cindro, N.; Kulcsár, M. J.; Tireli, M.; Užarević, K.; Bregović, N.; Tomišić, V. Protonation and Anion Binding Properties of Aromatic Bis-Urea Derivatives—Comprehending the Proton Transfer. *Chem. - Eur. J.* **2019**, *25*, 4695−4706.
(19) (a) Kubo, Y.; Ishihara, S.; Tsukahara, M.; Tokita, S. Isothiouronium-derived simple fluorescent chemosensors of anions. *J. Chem. Soc., Perkin Trans. 2* **2002**, *2*, 1455−1460. (b) Amendola, V.; Boiocchi, M.; Esteban-Gómez, D.; Fabbrizzi, L.; Monzani, E. Chiral receptors for phosphate ions. *Org. Biomol. Chem.* **2005**, *3*, 2632−2639. (c) Baggi, G.; Boiocchi, M.; Fabbrizzi, L.; Mosca, L. Moderate and Advanced Intramolecular Proton Transfer in Urea−Anion Hydrogen-Bonded Complexes. *Chem. - Eur. J.* **2011**, *17*, 9423−9439. (d) Mungalpara, D.; Kelm, H.; Valkonen, A.; Rissanen, K.; Keller, S.; Kubik, S. Oxoanion binding to a cyclic pseudopeptide containing 1,4-disubstituted 1,2,3-triazole moieties. *Org. Biomol. Chem.* **2017**, *15*, 102−113. (e) Gillen, D. M.; Hawes, C. S.; Gunnlaugsson, T. Solution-State Anion Recognition, and Structural Studies, of a Series of Electron-Rich meta-Phenylene Bis(phenylurea) Receptors and Their Self-Assembled Structures. *J. Org. Chem.* **2018**, *83*, 10398−10408. (f) Zhao, W.; Qiao, B.; Tropp, J.; Pink, M.; Azoulay, J. D.; Flood, A. H. Linear Supramolecular Polymers Driven by Anion−Anion Dimerization of Difunctional Phosphonate Monomers Inside Cyanostar Macrocycles. *J. Am. Chem. Soc.* **2019**, *141*, 4980−4989.
(20) Mungalpara, D.; Valkonen, A.; Rissanen, K.; Kubik, S. Efficient stabilisation of a dihydrogenphosphate tetramer and a dihydrogenpyrophosphate dimer by a cyclic pseudopeptide containing 1,4-disubstituted 1,2,3-triazole moieties. *Chem. Sci.* **2017**, *8*, 6005−6013.
(21) (a) Wood, R. H.; Platford, R. F. Free energies of aqueous mixtures of NaH_2PO_4 and $NaClO_4$: Evidence for the species $(H_2PO_4)_2^{-2}$. *J. Solution Chem.* **1975**, *4*, 977−982. (b) Rull, F.; Del Valle, A.; Sobron, F.; Veintemillas, S. Raman study of phosphate dimerization in aqueous KH_2PO_4 solutions using a self-deconvolution method. *J. Raman Spectrosc.* **1989**, *20*, 625−631. (c) Shaver, J. M.; Christensen, K. A.; Pezzuti, J. A.; Morris, M. D. Structure of Dihydrogen Phosphate Ion Aggregates by Raman-Monitored Serial Dilution. *Appl. Spectrosc.* **1998**, *52*, 259−264. (d) McNally, J. S.; Wang, X. P.; Hoffmann, C.; Wilson, A. D. Self-assembly of molecular ions via like-charge ion interactions and through-space defined organic domains. *Chem. Commun.* **2017**, *53*, 10934−10937.
(22) Barišić, D.; Tomišić, V.; Bregović, N. Acid-base properties of phosphoric and acetic acid in aprotic organic solvents − A complete thermodynamic characterisation. *Anal. Chim. Acta* **2019**, *1046*, 77−92.
(23) Consistent with previous studies (e.g., ref 19), the addition of a known percentage of water reduces the variablity of trace water content. For a description of the speciation, see SI-2.
(24) Price, W. S.; Tsuchiya, F.; Arata, Y. Lysozyme Aggregation and Solution Properties Studied Using PGSE NMR Diffusion Measurements. *J. Am. Chem. Soc.* **1999**, *121*, 11503−11512.
(25) Martin, R. B. Comparisons of Indefinite Self-Association Models. *Chem. Rev.* **1996**, *96*, 3043−3064.
(26) Lewin, L. *Polylogarithms and associated functions*; Elsevier: North Holland, NY, 1981.
(27) (a) Rajbanshi, A.; Wan, S.; Custelcean, R. Dihydrogen Phosphate Clusters: Trapping $H_2PO_4^-$ Tetramers and Hexamers in Urea-Functionalized Molecular Crystals. *Cryst. Growth Des.* **2013**, *13*, 2233−2237. (b) White, N. G. Antielectrostatically hydrogen bonded anion dimers: counter-intuitive, common and consistent. *CrystEngComm* **2019**, *21*, 4855−4858.
(28) See Supporting Information S7 for details of the binding constants. K_1 for *E*-**1** = 3.3 × 10^2 M^{-1}; K_1 for *Z*-**1** = 2.1 × 10^3 M^{-1}.
(29) Thordarson, P. Determining association constants from titration experiments in supramolecular chemistry. *Chem. Soc. Rev.* **2011**, *40*, 1305−1323.
(30) Cho, J.; Verwilst, P.; Kang, M.; Pan, J.-L.; Sharma, A.; Hong, C. S.; Kim, J. S.; Kim, S. Crown ether-appended calix[2]triazolium[2]-arene as a macrocyclic receptor for the recognition of the $H_2PO_4^-$ anion. *Chem. Commun.* **2020**, *56*, 1038−1041.
(31) Geometries calculated by DFT are given in the Supporting Information, SI-11.
(32) At 5 mM host concentrations used, and with K_1 of 360 and 2100 for *E*-**1** and *Z*-**1**, respectively, the proportion of unbound host is less than 5% with, respectively, 5.5 equiv and 2.5 equiv of $H_2PO_4^-$. See the Supporting Information, S9, for details.
(33) For example, $[H_2PO_4^-]$ = 50 mM, [**1**] = 5 mM: Table 1, entries 4−8; SI-8. See SI-7 for speciation curves based on measured K_a values.
(34) Viscosities of $[NBu_4][H_2PO_4]$ solutions in DMSO-d_6 were measured directly and fitted to a viscosity calibration curve, which was used to compensate for changes in measured *D* caused by viscosity. See the Supporting Information, S4, for details.
(35) Equivalent experiments using $[NBu_4][OAc]$ in place of $[NBu_4][H_2PO_4]$ do not result in similar changes in the measured *D* of the host, suggesting that the ability of $H_2PO_4^-$ to form extended hydrogen-bound chains is critical for the observed changes in measured *D* (see the Supporting Information, SI-8.2).
(36) Note that despite *E*-**1** having a lower measured K_1 for $H_2PO_4^-$ than Z-**1**, there is no free host left in both cases at 50 mM, see the Supporting Information, S9.
(37) This analysis does not rely on the accuracy of the isodesmic binding model and fitted parameters: the proposed $[H^{1-2}(G_n)_{2-3}]$ average structure only requires the experimentally measured effective $D(H_2PO_4)$. See the Supporting Information, S9, for details.
(38) Feldmeier, C.; Bartling, H.; Riedle, E.; Gschwind, R. M. LED based NMR illumination device for mechanistic studies on photochemical reactions − Versatile and simple, yet surprisingly powerful. *J. Magn. Reson.* **2013**, *232*, 39−44.
(39) (a) Urbańczyk, M.; Bernin, D.; Czuroń, A.; Kazimierczuk, K. Monitoring polydispersity by NMR diffusometry with tailored norm regularisation and moving-frame processing. *Analyst* **2016**, *141*, 1745−1752. (b) MacDonald, T. S. C.; Price, W. S.; Astumian, R. D.; Beves, J. E. Enhanced Diffusion of Molecular Catalysts is Due to Convection. *Angew. Chem., Int. Ed.* **2019**, *58*, 18864−18867. (c) MacDonald, T. S. C.; Price, W. S.; Beves, J. E. Time-Resolved Diffusion NMR Measurements for Transient Processes. *ChemPhysChem* **2019**, *20*, 926−930.
(40) (a) Swan, I.; Reid, M.; Howe, P. W. A.; Connell, M. A.; Nilsson, M.; Moore, M. A.; Morris, G. A. Sample convection in liquid-state NMR: Why it is always with us, and what we can do about it. *J. Magn. Reson.* **2015**, *252*, 120−129. (b) Barbosa, T. M.; Rittner, R.; Tormena, C. F.; Morris, G. A.; Nilsson, M. Convection in liquid-state NMR: expect the unexpected. *RSC Adv.* **2016**, *6*, 95173−95176.
(41) Ammann, C.; Meier, P.; Merbach, A. A simple multinuclear NMR thermometer. *J. Magn. Reson.* **1982**, *46*, 319−321.
(42) Some evidence also suggests that complexes involving two or more host molecules are selective for the same host isomer. Comparing *D*(*E*-**1**) and *D*(*Z*-**1**) for 5 mM solutions of pure isomers to those for 5 mM of a 1:1 mixture of the isomers, both isomers diffuse faster in the mixed solution (Table 1; entries 4, 5, and 7). The increase is small (2% for *D*(*E*-**1**), 4% for *D*(*Z*-**1**)), but a similar trend appears during time-resolved diffusion monitoring of photoswitching hosts (Fig. 6), where switching *Z*-**1** into *E*-**1** also causes a slight increase in *D*(*Z*-**1**) and a decrease in *D*(*E*-**1**).

https://dx.doi.org/10.1021/jacs.0c09072
J. Am. Chem. Soc. 2020, 142, 20014−20020